Available online at www.sciencedirect.com
SCIENCE DIRECT
Catalysis Today 105 (2005) 78–84
CATALYSIS TODAY
www.elsevier.com/locate/cattod

Nucleation and growth of 1B metal clusters on rutile TiO_2(1 1 0): Atomic level understanding from first principles studies

Devina Pillay, Yun Wang, Gyeong S. Hwang *

Department of Chemical Engineering, The University of Texas at Austin, Austin, TX 78712, USA

Abstract

Nanometer sized metal clusters dispersed on oxide supports often exhibit much higher activity than single-component metal catalysts. Their catalytic performance markedly depends on cluster size, shape and size distributions, along with support materials and support preparation methods. Supported metal nanoclusters can also easily rearrange and sinter during the course of thermally activated catalytic reactions even at moderate temperatures. An accurate assessment of the effects of cluster–support interactions on the growth, structure and reactivity of supported metal clusters, as well as the adsorbate-induced structural changes is therefore necessary to understand their catalytic performance under realistic operating conditions. The detailed understanding will also contribute to development of a new and reliable way to control their structural catalytic properties on the atomic scale. As a part of the effort to gain this atomic level understanding, we present our recent findings from density functional theory calculations, including: electronic structure of a reduced TiO_2(1 1 0) surface and interactions between oxygen vacancies, with a brief introduction to the dynamics of oxygen molecules on the reduced surface, role of oxygen vacancies and oxygen adspecies in the nucleation of Au, Ag and Cu clusters.

Keywords: Nanoclusters; Cluster–support; Adsorbate

1. Introduction

The synthesis and characterization of ''so-called'' nanoclusters within the size range of 1–10 nm has become a major interdisciplinary area of research over the last decade. Nanoclusters have distinctly different chemical and physical properties from their corresponding bulk counterparts. In particular, oxide supported metal nanoclusters have been found to exhibit high catalytic activity [1,2]. For instance, Au has long been known to be chemically inert in its bulk form, as compared to other transition metals [3]. It has, therefore, received little attention as a catalyst. However, nanometer size Au clusters dispersed on TiO_2 have been found to exhibit high activity for a variety of catalytic oxidation processes at or below room temperature [4]. The unusual catalytic activity appears to be a strong function of the cluster size; that is, only supported Au clusters in the range of 2–3 nm are very active [4,5]. Similarly, TiO_2-supported small Ag clusters (2–4 nm) also exhibit high catalytic activity and selectivity for propylene epoxidation and low-temperature CO oxidation [6] (while larger clusters are much less active [7]). These observations have lead to a speculation that there may exist a range of critical cluster sizes at which all metals exhibit unusual catalytic properties[8].

Due to weak cluster–support interfacial interactions, small metal clusters are easily rearranged and become unstable toward sintering in response to changes in the gaseous environment even at moderate temperatures [9–11]. This may lead to the loss of their catalytic activity, which is indeed a drawback of supported metal catalysts. An accurate assessment of adsorbate-induced structural changes, as well as growth mechanisms, is therefore necessary to better understand the catalytic properties and performance of supported metal clusters under realistic operation conditions. At present, many fundamental aspects of the nucleation, growth and sintering are poorly understood [4].

The dynamics of metal clusters will be largely determined by the atomic and electronic structure of oxide support

* Corresponding author. Tel.: +1 512 471 5238; fax: +1 512 471 7060.
E-mail address: gshwang@che.utexas.edu (G.S. Hwang).

0920-5861/$ – see front matter © 2005 Elsevier B.V. All rights reserved.
doi:10.1016/j.cattod.2005.04.016

surfaces. The cluster–support interactions also strongly influence the reactivity of metal clusters [5,12]. However, despite long lasting efforts, little is known about the interface properties of these systems [13]. This is primarily due to difficulties in direct characterization of buried interfaces. Over recent years, significant advances in computing power and theoretical methods have made it possible to explore metal cluster dynamics and metal–support interfacial interactions using first principles quantum mechanics calculations [14–16]. Such atomistic modeling can offer valuable insight into the growth, structure and properties of oxide-supported metal nanoclusters.

In this paper, we present our recent first principles studies of the structure and properties of reduced TiO_2(1 1 0) rutile surfaces; the role of oxygen vacancies in nucleation of 1B metal clusters on TiO_2(1 1 0); and the effect of oxygen adspecies on Au cluster nucleation on TiO_2(1 1 0). The surface properties of oxides can be modified by surface defects, dopant impurities and adsorbates, which will in turn alter physical and chemical processes occurring on the surfaces. Therefore, a detailed understanding of the complex interactions between defects, adsorbates and metal clusters will greatly contribute to accurate assessment of the performance of supported metal nanocatalysts under realistic process conditions and realization of the precise control of their catalytic properties by tailoring cluster size, shape and spatial distribution on the atomic scale.

Oxide supported Au, Ag and Cu nanoclusters often show markedly different physical and chemical characteristics. Recent experimental work [17], for instance, has shown that the Ag catalyst is almost inactive while the Cu and Au catalysts exhibit intermediate and very high activities in the water gas shift reaction, respectively. The comparative study of 1B metals is an important subject not only industrially, but also fundamentally.

2. Computational approach

Our quantum mechanics calculations are based on (spin-polarized) density functional theory (DFT) within the generalized gradient approximation (GGA) [18], as implemented in the VASP code [19,20]. We also calculate the adsorption properties of Au, Ag and Cu on the stoichiometric TiO_2(1 1 0) surface with the local spin density approximation (LSDA) with the Ceperly-Adler [21] form parameterized by Perdew and Zunger [22]. We use Vanderbilt type ultrasoft pseudopotentials [23,24] and plane-wave cut-off energy of 300 eV, which yields well-converged results. Charge densities are calculated using the residual minimization method-direct inversion of the interactive subspace (RMM-DIIS) algorithm, and atomic structures are optimized by minimizing the Hellman–Feymann forces using the conjugate gradient method.

The oxide surface considered here is modeled using a 9 or 15 atomic-layer slab that is separated from its vertical periodic image by a vacuum space of 17 Å. Here, the bottom layer is fixed at the bulk position, and all other substrate atoms and adsorbates are allowed to relax fully. In order to eliminate the interaction between adsorbates and their lateral periodic images, we use a rather large (2×3) surface unit cell, except for some cases as indicated later. For the Brillouin Zone integration, we use the ($2 \times 4 \times 1$) Monkhorst-Pack mesh of k points.

3. Results and discussion

3.1. Structure of TiO_2(1 1 0) rutile

The (1 1 0) rutile surface is the most thermodynamically stable among low-index TiO_2 surfaces. The stoichiometric surface consists of two types of Ti atoms and four types of O atoms: five-fold coordinated Ti(5c), six-fold coordinated Ti(6c), two-fold coordinated bridging O(2c), three-fold coordinated in-plane O(3c) and two other subsurface O atoms.

The TiO_2 surface usually contains a significant number of oxygen vacancies [25–27]. Recent theoretical studies have shown that the atomic and electronic structures of TiO_2(1 1 0) are markedly altered by the presence of oxygen vacancies [28,29]. While the properties of the stoichiometric surface are well understood [28–37], the formation, structure, energetics, dynamics and chemistry of surface defects are still unclear.

We examine a partially reduced surface that is constructed by removing a bridging O(2c) atom from a given surface cell. The formation of the completely reduced surface is unlikely [38,39], so we do not consider the case here. The Ti(6c) atoms adjacent to the O vacancy become five coordinated; denoted as $Ti(6c)_d$ hereafter. Fig. 1 shows the local density of states (LDOS) of neighboring Ti atoms, as indicated [40]. The significant shift of the 3d states (of not

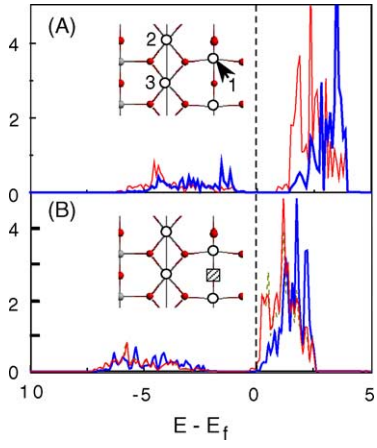

Fig. 1. LDOS of surface Ti atoms (A) on clean TiO_2(1 1 0) and (B) reduced TiO_2(1 1 0). The thick solid, thin solid and dotted lines, respectively, show LDOS plots of Ti atoms 1–3, as indicated. The small black balls represent rsurface O atoms and the white balls indicate surface Ti atoms.

Table 1
Oxygen vacancy formation energy (in eV) calculated using different sizes of the surface unit cell, as indicated

	E_f (eV)
(1 × 2)	6.91
(1 × 3)	5.84
(1 × 4)	5.59
(1 × 5)	5.38
(2 × 2)	6.93
(2 × 3)	5.49
(2 × 4)	5.37

only $Ti(6c)_d$ but also Ti(5c) neighboring atoms) towards the Fermi level suggests the delocalization of unpaired electrons from the vacancy site along the neighboring Ti rows. As a result, there exists an interaction between vacancies when they reside close by [41,42]. For a fully isolated neutral F_s center, however, we expect the excess electrons will largely be localized at the vacancy site by the inter-ionic Coulomb interaction [43].

To assess the vacancy–vacancy interaction, by varying the surface cell size we calculated the oxygen vacancy formation energy, $E_f(V)$, which is defined as

$$E_f(V) = E_{s-TiO_2} - E_{r-TiO_2} - E_o$$

where E_{s-TiO_2}, E_{r-TiO_2} and E_o are the total energies of the stoichiometric surface, the reduced surface, and a free O atom, respectively.

As listed in Table 1 [44], the formation energy decreases significantly as the surface cell size increases from (1 × 2) to (1 × 5) and from (2 × 2) to (2 × 4). This indicates the vacancy–vacancy interaction is repulsive in nature, suggesting the formation of O vacancy pairs and rows is energetically unfavorable as briefly mentioned earlier.

The reaction dynamics of gaseous reactants and products are often governed by O vacancies. For instance, molecular O_2 adsorbs on TiO_2(1 1 0) only when vacancies are present [45]. Surface bound oxygen species can in turn directly influence chemical and photochemical processes occurring on the reduced surface [46]. Recent experimental [27] and theoretical [40] studies have revealed interesting dynamical features of oxygen species associated with O vacancies. Included among these phenomena are: O_2 deposition on a reduced TiO_2(1 1 0) surface is more likely to mediate the movement of O vacancies, rather than healing O-vacancies completely, at low temperatures (<300 K); atomic O deposition may aggravate surface reduction (if O-vacancy density is not substantial) and O_2 mobility is directly related to the density of O vacancies. Despite the recent experimental and theoretical investigations, in many respects, the basic knowledge of surface defects, defect–adsorbate interactions, and their effects on surface properties is still lacking. Considering its importance in understanding not only the surface properties but also the growth, structure and reactivity of supported metal nanocatalysts, significant experimental and theoretical efforts should continuously be devoted to the investigation of the fundamental behaviors associated with defects and adsorbates.

3.2. Nucleation and growth 1B metal clusters on TiO_2

3.2.1. Role of oxygen vacancies

As shown earlier, the presence of oxygen vacancies on TiO_2(1 1 0) significantly alters the surface properties. This may in turn affect the adsorption and diffusion metal adatoms, and consequently metal cluster growth.

Fig. 2 shows the potential energy maps for a single Au adatom on the stoichiometric (a) and reduced (b) rutile TiO_2(1 1 0) surface [47]. The reduced surface contains one oxygen vacancy per periodic (2 × 3) surface cell which corresponds to a vacancy concentration of approximately 17%. On the stoichiometric surface we carefully sampled a (1 × 1) area by breaking it up into 60 evenly spaced points and calculated the adsorption energy after a full geometry optimization using a (4 × 4 × 1) k-point mesh. On the reduced surface, we broke up the (2 × 2) area into 700 evenly spaced points and after a full geometry optimization using a (2 × 4 × 1) k-point mesh we also calculated the adsorption energy. We then linearly interpolated energies between neighboring points to construct the potential energy surfaces.

On the stoichiometric surface, the most stable Au adsorption site is the four-fold hollow position over the Ti(5c) and the in-plane and bridging O(2c) atoms [41,42,44]. In fact, the Au adsorption energy varies insignificantly, ranging from 0.4 to 0.6 eV, except for the sites atop the in-plane O(3c) atoms which turns out to be the most unfavorable (noted by the energy peaks). This potential energy map clearly demonstrates there is no preferential diffusion direction for Au on the stoichiometric surface.

On the reduced surface, the most energetically favorable site (noted by the potential energy valley) is the oxygen vacancy site. In addition, we also find that there are several local energy minima (that correspond to the sites atop Ti(5c) atoms) on the neighboring Ti(5c) rows. Au adsorption energies at the sites atop Ti(5c) atoms are approximately 0.3 eV lower than at the vacancy site. This suggests that Au clusters may nucleate not only at O-vacancy sites but also at Ti(5c) sites at low temperatures, consistent with recent experimental observations by constant current topography scanning tunneling microscopy (CCT-STM) [48].

The calculated barrier for diffusion of Au along the Ti(5c) row is 0.41 eV. In comparison, Au atoms located perpendicular ([−1 1 0] direction) and along the bridging O row ([0 0 1] direction) are very unstable. Therefore, it is highly unlikely that an Au atom would diffuse out of the vacancy site onto the bridging O row. The significant increase in Au binding to Ti(5c) sites is evidently attributed to electron delocalization from the vacancy site. Our calculation results [47] show neither an adatom, a dimer, nor a trimer at the vacancy site can fully reoxidize the surface. Considering that in Au cluster formation a single O vacancy is likely to bind

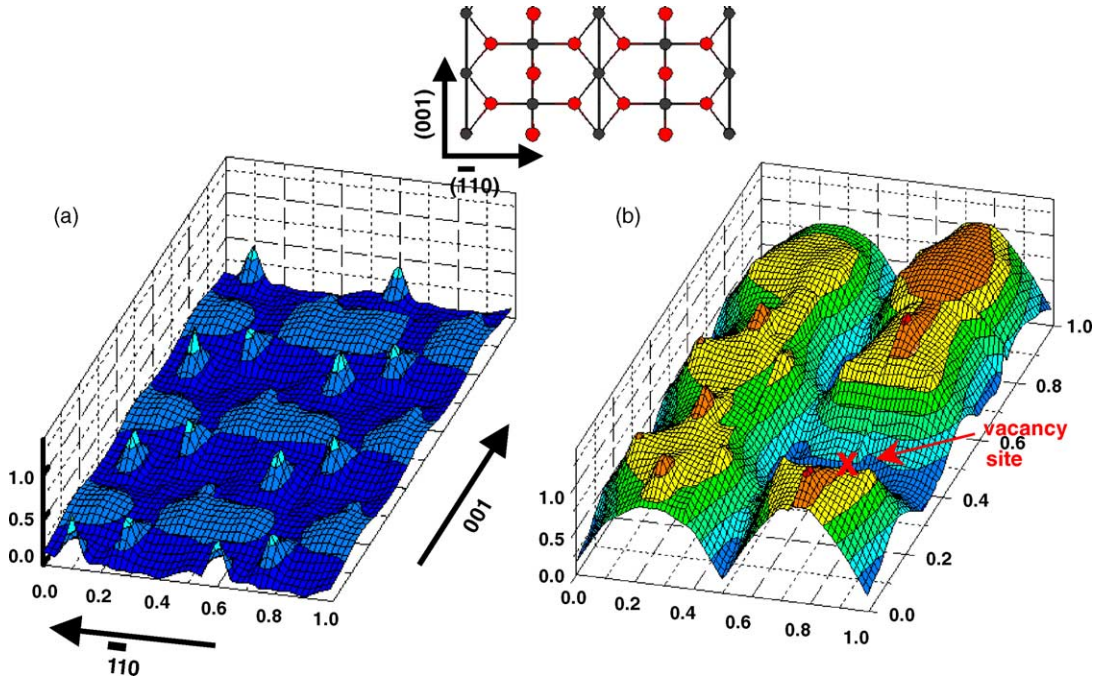

Fig. 2. Potential energy maps for a single Au atom on TiO_2(1 1 0): (a) stoichiometric and (b) reduced. The energy values are calculated with respect to the lowest energy at each (2 × 3) surface cell considered.

three Au atoms on average [49], we can expect that O vacancies could provide a low-barrier diffusion pathway along the Ti(5c) row. This directionality in Au adatom diffusion may be responsible for the formation of elongated Au particles in the [0 0 1] direction between bridging O(2c) rows at the early stages of growth (<0.1 ML), as evidenced by CCT-STM observations [48].

Fig. 3 shows the potential energy maps for a single Ag adatom on the stoichiometric (a) and reduced (b) rutile TiO_2(1 1 0) surface. The reduced surface contains one

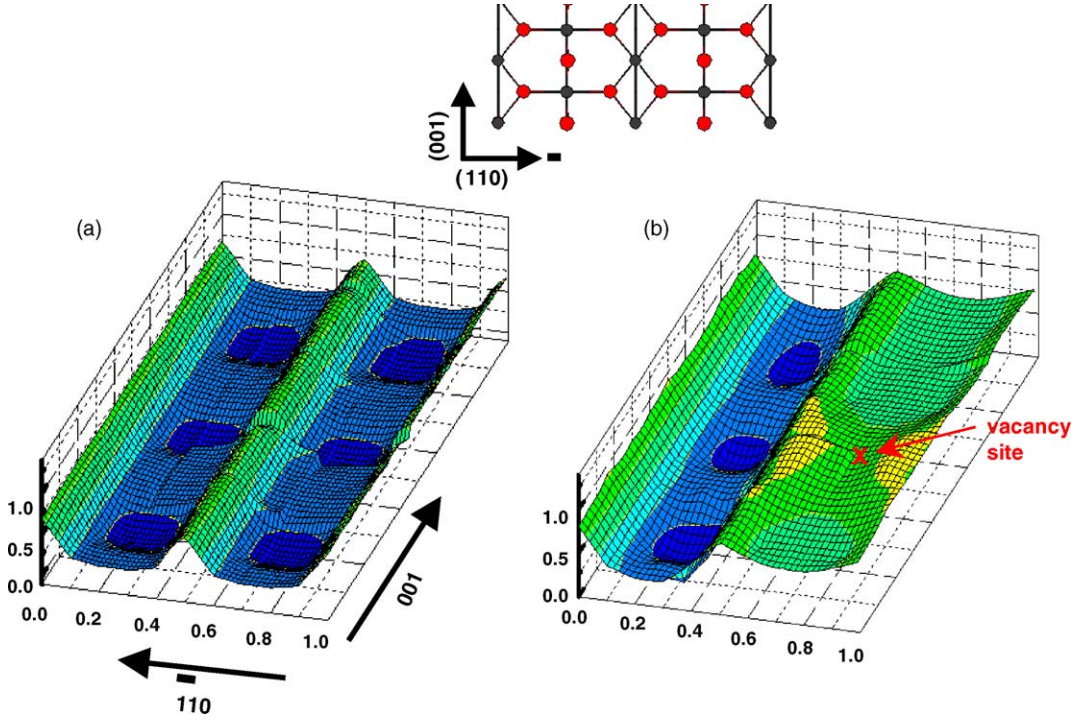

Fig. 3. Potential energy maps for a single Ag atom on TiO_2(1 1 0): (a) stoichiometric and (b) reduced. The energy values are calculated with respect to the lowest energy at each (2 × 3) surface cell considered.

oxygen vacancy per periodic (2 × 3) surface cell. Ag and Cu adatoms display similar trends on both stoichiometric and reduced surfaces, so here only the Ag case is presented.

The most favorable adsorption site for Cu and Ag on the stoichiometric surface is in between two bridging oxygen atoms along the bridging oxygen row in the [0 0 1] direction. The adsorption energies decrease with an increase in distance from the O(2c) atoms, and are in the ranges of 1.20–1.60 eV for Ag and 1.10–2.58 eV for Cu. Similar adsorption behavior is predicted by Giordano et al. [39] using DFT-GGA cluster and slab calculations. They also found that Ag and Cu interact favorably with O(2c) atoms, but their adsorption energies ranges differ for Ag (0.34–2.30 eV) and Cu (0.55–2.67 eV) from our results. On the stoichiometric surface, the potential energy map (Fig. 3(a)) indicates that there is a distinctive energy minimum pathway along the [0 0 1] direction (bridging oxygen row). The difference in energy between the [0 0 1] directions versus the [−1 1 0] direction is approximately 0.70 eV.

We calculated a diffusion barrier of 0.36 and 0.78 eV for Ag and Cu, respectively, to diffuse from the site between two bridging oxygen atoms to the site atop bridging oxygen. The lower adsorption energies and diffusion barriers for Ag, relative to Cu, can be understood given its lower oxygen affinity and lower heat of oxide formation than Cu [13]. These results are consistent with recent STM measurements [50] that show Cu clusters are on average smaller in size than Ag clusters due largely to the mobility difference between Cu and Ag adatoms.

From the potential energy map on the reduced TiO_2(1 1 0) surface (Fig. 3(b)) [51] it is obvious that formation of an oxygen vacancy drastically affects the diffusion and adsorption behavior of Ag. The bridging O row containing the vacancy and the neighboring Ti(5c) rows become highly unfavorable for Ag adsorption. Since vacancies are energetically unlikely to neighbor each other, between two vacancies there likely exists sites where the adsorption of a Ag/Cu adatom would be favorable. That is, at these sites an Ag/Cu adatom could be trapped. Thus, the density of clusters can be directly proportional to that of O vacancies, consistent with experimental observations [50,52].

As a whole, our calculation results suggest that a single O vacancy acts as a diffusion barrier for Ag and Cu adatoms along the bridging O row, while it serves as a nucleation center for an Au cluster.

3.2.2. Role of oxygen species

During oxidation processes, oxygen species can compete with Au atoms for O vacancy sites, and they can also alter support properties, metal–metal interactions and cluster–support interactions. This may in turn significantly affect the nucleation, growth and sintering of Au clusters. Here, we examine the interaction of oxygen species with small Au clusters.

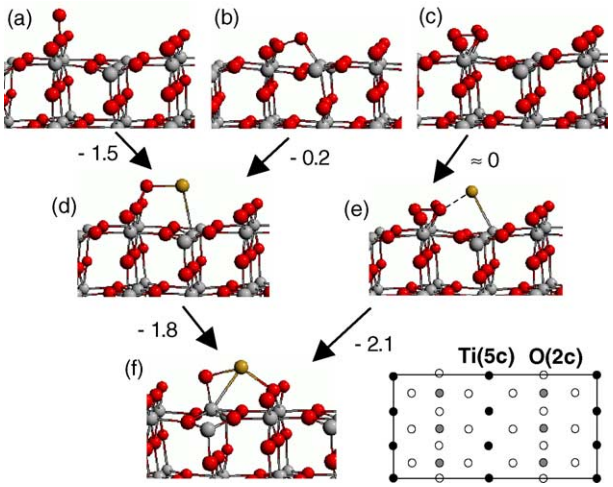

Fig. 4. Molecular oxygen adsorbed on an oxygen vacancy defect in three different configurations: (a) perpendicular, (b) inclined and (c) parallel. Interactions of an Au atom with the adsorbed oxygen molecule (d and e). An Au–O complex bound to TiO_2(1 1 0) (f); it may be formed by Au-catalyzed O_2 dissociation at the vacancy site (d or e) or by direct pairing of mobile Au and O adatoms. Energy changes (in eV) for different states are indicated (the negative signs indicate energy gain). Here, the energy of an Au adatom is set to be zero. The red, gray and yellow balls represent O, Ti and Au atoms, respectively. The inset shows the top view of the (2 × 3) unit cell used in this work. (For interpretation of the references to colour in this figure legend, the reader is referred to the web version of the article.)

First, we look at the effect of O_2 termination of O vacancies on Au cluster nucleation. We consider three different adsorption states of O_2 at the vacancy site, as shown in Fig. 4, including: (a) perpendicular, (b) inclined and (c) parallel to the surface. All three configurations turn out to be stable with adsorption energies greater than 1.0 eV. The inclined and parallel states are energetically comparable, with a barrier of about 0.4 eV for transforming between the two configurations. The perpendicular state is more than 1 eV less stable than the inclined and parallel states. Our calculation predicts there is no sizable barrier for the transformation of the perpendicular state into the inclined state.

Notice that, compared to 1.24 Å for neutral O_2, the O–O bond length of the adsorbed O_2 increases to 1.35, 1.47 and 1.48 Å in the perpendicular, inclined, and parallel cases, respectively. This is due to electron transfer to the adsorbed O_2 from the surface. The values of 1.35 and 1.47 (1.48) Å are very close to 1.33 Å of $(O–O)^-$ anion (from HO_2) and 1.46 Å of $(O–O)^{2-}$ anion (from H_2O_2), respectively [53], suggesting that approximately one electron is transferred to the perpendicular state and two electrons to the inclined and parallel states.

When Au is positioned near parallel O_2 (Fig. 4(d)), there is virtually no energy difference between the before and after Au–O_2 complex formation [= E(Au/s–TiO_2) + E(O_2/r–TiO_2) − E(Au–O_2/r–TiO_2) − E(s–TiO_2), where Au/s–TiO_2 indicates Au on stoichiometric TiO_2, O_2/r–TiO_2 and Au–O_2/r–TiO_2 are O_2 and Au on reduced TiO_2, respectively, and s–TiO_2 is stoichiometric TiO_2 surface. When Au approaches

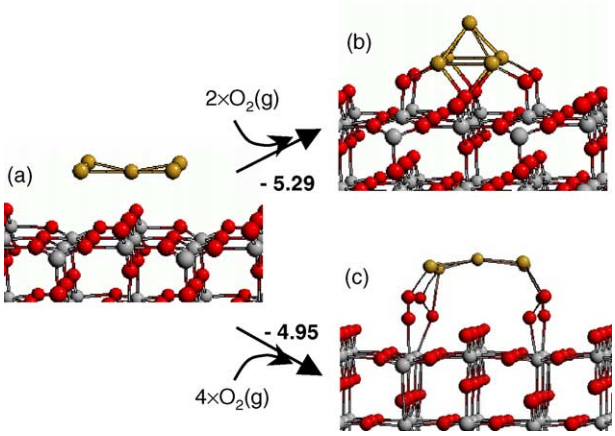

Fig. 5. (a) Au_5 particle, (b) Au_5 particle pinned by O atoms and (c) Au_5 particle pinned by O_2 molecules. The energy gains (in eV) by the Au–O complex formation are indicated. The red, gray and yellow balls represent O, Ti and Au atoms, respectively. (For interpretation of the references to colour in this figure legend, the reader is referred to the web version of the article.)

to inclined O_2, the top O atom interacts more strongly with Au than Ti(5c), leading to the Ti(5c)–Au–O–O configuration (Fig. 4(e)). The Au–O_2 complex formation lowers the total energy by ≈0.2 eV. When Au is placed near the perpendicular O_2, the top O atom leans toward the Au to form the Ti(5c)–Au–O–O configuration (Fig. 4(d)). Here, we can expect that the liberation of Au would leave the inclined O_2 behind, rather than the perpendicular O_2. In this case, the Au binding energy is approximated to be ≈0.2 eV. The small Au binding energies suggest that O_2-terminated vacancies are no longer an active nucleation site for Au clusters, although O_2 adsorption does not fully reoxidize the surface [41].

Next, the results shown in Fig. 5 suggest oxygen species can contribute to stabilizing small Au clusters. Here, we consider a five-atom particle (Au_5). The Au_5 adsorption energy is estimated to be nearly 0 eV (Fig. 5(a)). When four oxygen atoms (Fig. 2(b)) are placed at the periphery of Au_5, the edge Au atoms become ionized to form a strong ionic bond with the bridging O(2c) (Fig. 5(b)). The resulting energy gain of Au_5O_4 [Au_5O_4/s–TiO_2], relative to the Au_5 particle [Au_5/s–TiO_2] and two gas-phase O_2 molecules [$2 \times O_2$(g)], is estimated to be about 5.29 eV [= E(Au_5O_4/s–TiO_2) − E(Au_5/s–TiO_2) − E($2 \times O_2$(g))]! We also place O_2 molecules at the periphery of Au_5 (Fig. 4(c)), showing the significant stabilization of Au_5 particle with the energy gain of 4.95 eV. These results demonstrate small Au particles (which may be nucleated mostly by O vacancies) can be stabilized further via the *oxygen pinning*. They also indicate oxygen species can be strongly bound to the periphery of (thin) small Au clusters. This is consistent with recent experimental observations that suggest atomic oxygen could bind to the surface more strongly in the presence of small Au clusters [54].

Adsorbates may significantly influence the structure and sintering of supported metal clusters. For instance, upon exposure to O_2, the sintering of Cu [55] and Ag [56] is enhanced and the structure of Cu changes from three- to two-dimensional. Ostwald ripening of Ag and Cu clusters is thought to be attributed to the formation of Ag_2O and Cu_2O complexes, which may decrease metal–metal binding energies and in turn facilitate the inter-cluster transport [55,56]. At present, however, many fundamental aspects of adsorbate-induced changes in metal cluster growth, structure and sintering are not fully understood. This warrants further investigations into the complex interactions between metal clusters, surface defects and adsorbates. The fundamental study will also assist in understanding the unusual catalytic properties of supported metal nanoclusters.

4. Summary

Based on density functional theory slab calculations we present: electronic structure of a reduced TiO_2(1 1 0) rutile surface, oxygen vacancy formation and vacancy–vacancy interaction on TiO_2(1 1 0) surface, role of oxygen vacancies in Au, Ag and Cu nucleation and effect of oxygen adspecies on Au cluster nucleation. We also briefly discuss the structure and dynamics of molecular oxygen on a reduced surface and adsorbate-induced changes in the growth, structure and sintering have supported Au, Ag and Cu clusters.

Firstly, removal of a neutral bridging O(2c) atom leaves two unpaired electrons that delocalize over Ti(5c) neighbors along the Ti rows. The delocalization extends beyond the fourth neighboring O(2c) sites to a great extent. As a result, there exists a strong interaction between vacancies when they reside close by. DFT calculation results suggest that the vacancy–vacancy interaction is repulsive in nature, implying the formation of O vacancy pairs and rows are energetically unfavorable.

Secondly, on the stoichiometric surface, the Au adsorption energy varies insignificantly, ranging from 0.4 to 0.6 eV, except for the sites atop in-plane O(3c) atoms. On the other hand, the most favorable adsorption site for Cu and Ag on the stoichiometric surface is in between two bridging oxygen atoms along the bridging oxygen row. The adsorption energies decrease with an increase in distance from the bridging O(2c) atoms, and are in the ranges of 1.20–1.60 eV for Ag and 1.10–2.58 eV for Cu. The presence of oxygen vacancies alters greatly the adsorption of diffusion of Au, Ag and Cu adatoms. Overall, our calculation results suggest that a single O vacancy serves as a nucleation center for Au cluster while acting as a diffusion barrier for Ag and Cu adatoms along the bridging O row. In addition, the electron delocalization from the vacancy site provides a low-energy diffusion path for Au adatoms along the neighboring Ti(5c) rows, with a barrier of 0.41 eV. We also find there are local energy minima at the sites atop Ti(5c) atoms, approximately 0.3 eV energetically less favorable than the vacancy site. These results could explain experimental

observations including: why the density of Au, Ag and Cu clusters is directly proportional to that of O vacancies; why Au particles are likely to nucleate not only at O-vacancy sites but also at Ti(5c) sites; why Au clusters form elongated in the [0 0 1] direction between bridging O(2c) rows at the early stages of growth (<0.1 ML) and why Cu clusters are on average smaller in size than Ag clusters.

Thirdly, molecular oxygen efficiently passivates oxygen vacancy defects on rutile TiO_2(1 1 0), suggesting that the O_2-terminated defect site is no longer an active nucleation site for Au particles. We also find that oxygen species are likely to contribute greatly to the immobilization of small Au particles by inducing strong ionic interactions with TiO_2(1 1 0).

While current experimental techniques are still limited to providing complementary real space information, using the combination of experiment and atomistic modeling we can gain many valuable insights into the growth, structure and properties of oxide-supported metal nanoclusters. Furthermore, by incorporating the fundamental understanding and data into larger scale simulations we can develop a multiscale computational model capable of not only explaining experimental observations but also predicting new structural and catalytic properties at various process conditions. The development of such multiscale model is underway in our group, by integrating various state-of-the-art theoretical techniques including: first principles quantum mechanics, molecular dynamics and metropolis/kinetic Monte Carlo.

Acknowledgements

The authors acknowledge the Welch Foundation (Grant No. F-1535) for their financial support of this work. All our calculations were performed using Cray-Dell Linux cluster and IBM Power4 system in Texas Advanced Computing Center (TACC) at the University of Texas at Austin. We thank Professor C.B. Mullins for critical reading of this manuscript and helpful discussion.

References

[1] A.T. Bell, Science 299 (2003) 1688.
[2] A.K. Santra, D.W. Goodman, J. Phys. : Condens. Matter 15 (2003) 31.
[3] B. Hammer, J.K. Norskov, Surf. Sci. 343 (1995) 211.
[4] M. Haruta, Catal. Today 36 (1997) 153.
[5] M. Valden, X. Lai, D.W. Goodman, Science 281 (1998) 1647.
[6] A.L. de Oliveira, A. Wolf, F. Schuth, Catal. Lett. 73 (2001) 157.
[7] T. Hayashi, K. Tanaka, M. Haruta, J. Catal. 178 (1998) 566.
[8] T.V. Choudhary, D.W. Goodman, Top. Catal. 21 (2002) 25.
[9] A. Kolmakov, D.W. Goodman, Catal. Lett. 70 (2000) 93.
[10] A. Kolmakov, D.W. Goodman, Surf. Sci. 490 (2001) 597.
[11] C.T. Campbell, S.C. Parker, D.E. Starr, Science 298 (2002) 811.
[12] P.L. Hansen, J.B. Wagner, S. Helveg, J.R. Rostrup-Nielsen, B.S. Clausen, H. Topsoe, Science 295 (2002) 2053.
[13] C.T. Campbell, Surf. Sci. Rep. 27 (1997) 1.
[14] C. Verdozzi, D.R. Jennison, P.A. Schultz, M.P. Sears, Phys. Rev. Lett. 82 (1999) 799.
[15] A. Christensen, E.A. Carter, J. Chem. Phys. 114 (2001) 5816.
[16] D.J. Siegel, L.G. Hector, J.B. Adams, Phys. Rev. B 65 (2002) 085415.
[17] F. Boccuzzi, A. Chiorino, M. Manzoli, D. Andreeva, T. Tabakova, L. Ilieva, V. Iadakiev, Catal. Today 75 (2002) 169.
[18] J.P. Perdew, J.A. Chevary, S.H. Vosko, K.A. Jackson, M.R. Pederson, D.J. Singh, C. Fiolhais, Phys. Rev. B 46 (1992) 6671.
[19] G. Kresse, J. Hafner, Phys. Rev. B 47 (1993) 558.
[20] G. Kresse, J. Furthmuller, Phys. Rev. B 54 (1996) 11169.
[21] D.M. Ceperley, B.J. Alder, Phys. Rev. Lett. 45 (1980) 566.
[22] J.P. Perdew, A. Zunger, Phys. Rev. B 23 (1981) 5048.
[23] D. Vanderbilt, Phys. Rev. B 41 (1990) 7892.
[24] G. Kresse, J. Hafner, J. Phys. :Condens. Matter 6 (1994) 8245.
[25] H. Onishi, Y. Iwasawa, Surf. Sci. 313 (1994) 783.
[26] P.W. Murray, N.G. Condon, G. Thornton, Phys. Rev. B 51 (1995) 10989.
[27] R. Schaub, E. Wahlstrom, A. Ronnau, E. Laegsgaard, I. Stensgaard, F. Besenbacher, Science 299 (2003) 377.
[28] P.J.D. Lindan, N.M. Harrison, M.J. Gillan, J.A. White, Phys. Rev. B 55 (1997) 15919.
[29] T. Bredow, G. Pacchioni, Chem. Phys. Lett. 355 (2002) 417.
[30] P. Reinhardt, B.A. Hess, Phys. Rev. B 50 (1994) 12015.
[31] U. Diebold, J.F. Anderson, K.O. Ng, D. Vanderbilt, Phys. Rev. Lett. 77 (1996) 1322.
[32] Q. Guo, I. Cocks, E.M. Williams, Phys. Rev. Lett. 77 (1996) 3851.
[33] G. Charlton, et al. Phys. Rev. Lett. 78 (1997) 495.
[34] S.P. Bates, G. Kresse, M.J. Gillan, Surf. Sci. 385 (1997) 386.
[35] C.L. Pang, S.A. Haycock, H. Raza, P.W. Murray, G. Thornton, O. Gulseren, R. James, D.W. Bullett, Phys. Rev. B 58 (1998) 1586.
[36] R.A. Bennett, P. Stone, N.J. Price, M. Bowker, Phys. Rev. Lett. 82 (1999) 3831.
[37] K.O. Ng, D. Vanderbilt, Phys. Rev. B 56 (1997) 10544.
[38] A. Bogicevic, D.R. Jennison, Surf. Sci. 515 (2002) 481.
[39] L. Giordano, G. Pacchioni, T. Bredow, J.F. Sanz, Surf. Sci. 471 (2001) 21.
[40] Y. Wang, D. Pillay, G.S. Hwang, Phys. Rev. B 70 (2004) 193410.
[41] Y. Wang, G.S. Hwang, Surf. Sci. 542 (2003) 72.
[42] A. Vijay, G. Mills, H. Metiu, J. Chem. Phys. 118 (2003) 6536.
[43] A.M. Ferrari, G. Pacchioni, J. Phys. Chem. 99 (1995) 17010.
[44] D. Pillay, Y. Wang, G.S. Hwang, Korean J. Chem. Eng. 21 (2004) 537.
[45] M.A. Henderson, W.S. Epling, C.L. Perkins, C.H.F. Peden, U. Diebold, J. Phys. Chem. B 103 (1999) 5328.
[46] M.A. Fox, M.T. Dulay, Chem. Rev. 93 (1993) 341.
[47] D. Pillay, G.S. Hwang, in press.
[48] F. Cosandey, T.E. Madey, Surf. Rev. Lett. 8 (2001) 73.
[49] E. Wahlstrom, N. Lopez, R. Schaub, P. Thostrup, A. Ronnau, C. Africh, E. Laegsgaard, J.K. Norskov, F. Besenbacher, Phys. Rev. Lett. 90 (2003) 026101.
[50] J.E. Reddic, J. Zhou, D.A. Chen, Surf. Sci. 494 (2001) 767.
[51] D. Pillay, G.S. Hwang, in press.
[52] K. Luo, T.P. St Clair, X. Lai, D.W. Goodman, J. Phys. Chem. B 104 (2000) 3050.
[53] C. Shu, N. Sukumar, C.P. Ursenbach, J. Chem. Phys. 110 (1999) 10539.
[54] V.A. Bondzie, S.C. Parker, C.T. Campbell, J. Vac. Sci. Technol. A-17 (1999) 1717.
[55] J. Zhou, Y.C. Kang, D.A. Chen, J. Phys. Chem. B 107 (2003) 6664.
[56] X.F. Lai, T.P. St Clair, D.W. Goodman, Faraday Discuss. (1999) 279.